

Resolving of typical intra system EMI coupling problems of an Inertial Sensor and Differential Capacitive Accelerometer – A Case Study

Devender^a, VV Rama Sarma^a, Rakesh Kichouliya^a, B. Chattopadhyaya^b, Satyajeet Singh^b, K.C.Das^b, Sweta Padma Mishra^b, Narasimha Reddy^c, G. Ravi^d, and MSY Siva Prasad^d
^aEMI/EMC Centre, ^bELOIRA, ^cISG, ^dMEMS Technology Centre, Research Centre Imarat, Vignyanakancha, Hyderabad – 500 069, Andhra Pradesh, India.
Fax: +91 040 24306240, 2459 7633, 24306553

ABSTRACT

The purpose of this paper is to discuss the Electromagnetic Interference (EMI) coupling problems encountered during the design and development of an Inertial Sensor (Ring Laser Gyro) and Differential Capacitive Accelerometer (MEMS based) for airborne applications. It explains the intra system EMI sources like, low frequency magnetic field and static voltage and interfering / coupling within the electronic packages, their adverse effects on the performance of the equipment, and the observations made during functional checks at the work centers. Also gives the detailed analysis / systematic approach followed for resolving these problems separately, as Case Study I and II by implementing simple and cost effective solutions with minor or no changes in the design requirements, which helped to achieve the Electromagnetic Compatibility (EMC) requirement in both electronic packages.

Key words: EMI, EMC, RLG, PDA, MEMS

1. INTRODUCTION

The inertial sensors like gyros and the accelerometers are very critical and important subsystems in inertial navigation for measuring the states of a missile system. These electronic subsystems are very sensitive to the Electromagnetic Environmental Effects, like EMI, EMV, ESD, etc. It is very essential to design these electronic packages to withstand these adverse effects of Electromagnetic environment from the day it is conceptualized for safe and reliable operation of mission. In this paper the authors want to share their experiences in resolving the typical EMI coupling problems aroused during the design and development of these airborne subsystems, as case study. The problem of each subsystem has been considered separately, as Case Study I and Case Study II.

The low frequency magnetic field generated by dither drive amplifier is coupled into Photo Detector Amplifier (PDA) circuit within the gyro electronics (Ring Laser Gyro - RLG) and its effects on performance of gyro RLG have been considered as **Case Study I**. Under this it is explained the principle of operation, functional test set up, measured test results, observations, analysis and a systematic approach followed to resolve the problem, by implementing appropriate EMI control techniques, without any major change in the design part. Similarly, the static voltage coupling problem and its adverse effects on the performance of Differential Capacitive Accelerometer have been explained in detail as **Case Study II**.

2.0 INERTIAL SENSOR / RING LASER GYRO (RLG) - CASE STUDY I

2.1 Principle of operation

The RLG is an Inertial Sensor that provides an output frequency proportional to inertial angular rate about its sensitive axis. The ELG is an optical laser gyro whose working principle is based on Sagnac Effect [1, 2]. In RLG the cavity is of a ring configuration. The laser used is He³ – Ne^{20,22} type, which produces a beam of wavelength (λ) of 0.6328 μm . The two beams move in opposite directions – one in the clockwise direction, and the other in the counter clockwise direction. These two oppositely directed beams can be considered as traveling waves and the oscillation frequency of each is determined by the optical path length of the cavity. Thus in the RLG a small path length difference is translated into a more readily measurable frequency difference (beat frequency) to find out the body rotational information. The signal generated from the RLG is processed electronically. A schematic diagram depicting the laser block and its associated electronics is mentioned in figure.1.

The lasing action is initiated through, a high voltage pulse of the order of 15kV for a duration of 1.5 μs applied through a light-up transformer and its electronics. Thereafter, the lasing is sustained by means of High Frequency Oscillator (HFO). The signal of RLG is fed to a photodiode which generates a current signal of the order of 30 nano amps. A photo

detector amplifier (PDA) of trans-impedance type is employed to convert and amplify the photodiode signal to an appreciable voltage level.

Optical Block is dithered clockwise and anticlockwise with respect to the RLG sensitive axis at its natural resonance frequency. A Dither Drive Card along with Voltage Converter Card is used for this purpose. The output of the dither drive electronics is provided to the piezo-plates of torsion bars which assist the optical block in dither state enabling the RLG to overcome lock-in problem and thereby assists in detecting small rotational rates.

The RLG being an Active System, the heat generated due to discharge will cause variation in the refractive indices of the media and associated optics. These variations not only result in noise but also cause variations in the path of laser beams. Therefore, in order to compensate these variations, a heating mechanism is provided to one of the arms of the cavity to generate thermal radiation. The variation in path length is controlled by electronics. The control device electronics provide the required power to the HFO and Heater Assembly.

The Commutator Card, ELI05 Card and Host Card are the electronics used to control and sustenance of laser; and also to process the laser output Signal to extract inertial rotational information in terms of pulse. The interface for RLG is based on RS422 standard. A schematic diagram of functional test set up along with the interface is shown in the figure. 2.0. The output of the RLG is monitored by means of PC with Data Acquisition Software.

2.1 Specifications of RLG

Input

Rotational Rate

- (a) Maximum Rotational Rate : $\pm 300^0/\text{sec}$
- (b) Minimum Rotational Rate : $\pm 0.01^0/\text{Hr}$.

Scale Factor

- Scale Factor Value : $1.16 \pm 0.05 \text{ arc.sec} / \text{pulse}$
- Scale Factor Temperature Coefficient : 10 ppm
- Scale Factor Permissible Error
- (i) Non Linearity : 10 ppm
- (ii) Stability : 10 ppm
- (iii) Asymmetry : 10 ppm
- (iv) Repeatability : 5 ppm

Output

- (a) For Maximum Rotational Rate : $930000 \pm 41000 \text{ pulses} / \text{sec}$.
- (b) For Minimum Rotational Rate : $32 \pm 2 \text{ pulses} / \text{Hr}$.

Accuracy

- (a) Bias : $\leq 0.6^0 / \text{Hr}$
- (b) Bias Temperature Coefficient : $\leq 0.01^0 / \text{Hr}^0\text{C}$

Drift

- (a) Random Walk : $0.003^0 / \sqrt{\text{hr}}$
- (b) Bias Instability Coefficient : $0.01^0 / \text{hr}$

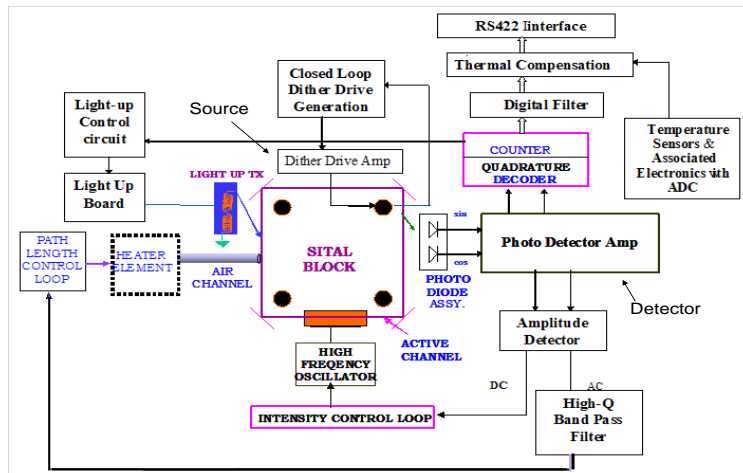


Figure. 1 A Schematic diagram of RLG depicting optical block and electronics

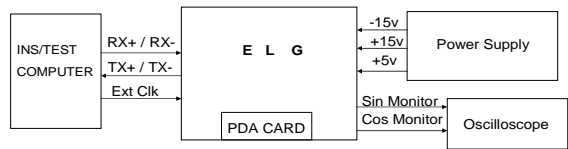


Figure. 2.0. Functional test configuration of RLG

2.2 Functional test and Test results

The functional test configuration of RLG is as shown in figure 2.0. The output parameters like drift and bias are monitored and sine, cosine signal voltage waveforms are captured on oscilloscope and as shown in figure 3.0. The sine and cosine signals are superimposed with the unwanted noise signals over the required voltage 4 Vp-p and a large variation in the bias and drift also observed. The noise signal voltage is also captured on oscilloscope is shown in figure 4.0, which is 700 mVp-p. The measured numerical values of parameters are exceeding the acceptable limits as shown in Table 1.

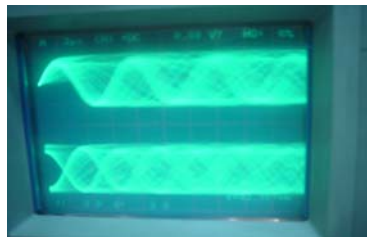


Figure 3. Sine and Cosine Signal waveforms monitored on the oscilloscope

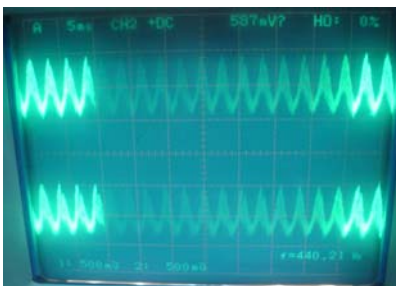


Figure 4. Noise Signals monitored on the oscilloscope

Table 1.0

Parameter	Signal + Noise	Noise
Sine Signal	4.7 Vp-p	700 mVp-p
Cosine Signal	4.7 Vp-p	700 mVp-p

2.3 Observations and Analysis

The following observations are noted under the above functional test configuration.

- a) The gyro output parameters like, rotational rate, bias and drift are found unstable and glitches are also observed
- b) The variation in the output of gyro is larger than the acceptable levels, i.e., $\pm 0.8^\circ$ Hr/gauss (2 pulses) is permissible.
- c) The noise signal is observed at the input of the photo detector amplifier and coupling into this high gain current amplifier (gain is $10V/\mu A$)
- d) The sine and cosine signal and noise voltages measured on the oscilloscope is 4.7 V peak to peak
- e) The frequency of coupled noise signal is 400 Hz
- f) The source of this frequency was the dither drive generator operating at 400 Hz, 90 Vp-p, and quasi square. This signal is being radiated and coupled into the PDA circuit.
- g) These are the very low frequency magnetic fields generated by the dither drive generator.
- h) It is observed that the dither drive generator is very close to the PDA and it is mounted below the laser cavity.
- i) It is found that, when the oscilloscope probe is taken near to PDA PCB card the noise signals are being picked up by the probe.
- j) It is also observed that the intensity of noise signal decreased drastically by about 300 – 400 mV when the oscilloscope probe is moved away from the PDA circuit
- k) It is identified that the signals radiated by the dither drive generator, are coupled into the PDA circuit and effecting on the output performance of the gyro
- l) The PDA circuit is directly exposed to these radiated fields and picking up these noise signals, since it was not enclosed in any metallic enclosure.
- m) As a quick fix measure the PDA circuit and the laser cavity torsion case is covered with a conductive copper foil tape of 3mil thickness and observed that there is an appreciable improvement (i.e., noise reduced to < 400 mV) in the output performance of the gyro.
- n) Further analysis, the orientation of the PDA circuit is changed by 180 degrees and observed much better performance than the earlier (i.e., noise reduced to < 200 mV).
- o) Finally, the PDA circuit was covered with high permeable Mu-metal sheet and found the further improvement (very close to the permissible level i.e., < 50 mV) in the output performance of the unit.

2.4 EMI Control Techniques (Solutions)

After analyzing the problem thoroughly the following EMI hardening techniques are implemented on permanent basis to overcome the coupling of unwanted noise signals, which are affecting the normal performance of gyro.

- a) The PDA circuit (PCB Card) is enclosed in a magnetically shielded box, since the coupling signal is identified as the magnetic field.
- b) Mu – metal sheet of 0.5 mm thickness with very high permeability in the order of 50 – 60 thousand is used for enclosure to suppress / attenuate the noisy magnetic fields as shown in figure 5 below.

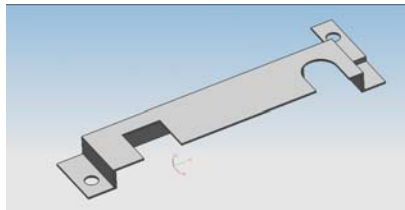


Figure 5. PDA Card Enclosure

- c) The metallic enclosure of PDA circuit is properly grounded to the main chassis of gyro.
- d) The chassis of RLG is made fully conductive, to improve the conductivity between chassis and ground.

2.5 Test Results after EMI hardening

After implementing the above solutions, the functional performance test of RLG is carried out and the results are very much encouraging and with in the acceptable / permissible limits, i.e., noise signal reduced to < 10 mV, over the required sine and cosine signals and the glitches are also suppressed fully. The output plots for both sine and cosine signals and

noise signals captured on the oscilloscope are shown in figures 6 and 7 and the numerical values are also given in Table 2.0. The improvement achieved in terms of attenuation is 36.9 dB.

E1 = 700 mV (noise voltage before EMI hardening), and
 E2 = 10 mV (noise voltage after EMI hardening)

$$\text{Attenuation in dB} = 20 \log E1/E2 = 20 \times \log (700\text{mV}/10\text{mV}) = 36.9$$

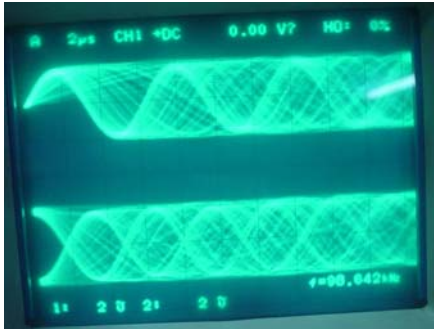


Figure 6. Sine and Cosine signals after EMI hardening



Figure 7. Noise Signal Coupled after EMI Hardening

Table 2.0

Parameter	Signal + Noise	Noise
Sine Signal	4.0 Vp-p	< 10mVp-p
Cosine Signal	4.0 Vp-p	< 10 mVp-p

3. DIFFERENTIAL CAPACITIVE MEMS ACCELEROMETER - CASE STUDY I I

3.1 Principle of operation

Micro Electro Mechanical Systems (MEMS) are devices that have static or movable components with some dimensions on the scale of microns. The differential capacitive MEMS accelerometer is a three plate parallel structure forming two capacitors with middle electrode (plate) common to both capacitors. The top and bottom electrodes / plates are fixed with middle plate / proof mass such that gap between the electrodes is same which is in the order of few microns. The nominal capacitance between top plate and proof mass C_1 and the capacitance between bottom plate and proof mass C_2 are equal. The accelerometer can be modelled as a simple spring-mass system consists of proof mass (middle electrode) supported by flextural beams. These structures are fabricated using well established semiconductor technology used in silicon IC industry, along with silicon bulk micro machining techniques using KOH and anodic wafer bonding [3].

The differential capacitive MEMS accelerometer works on the principle of complementary changes of two capacitors with respect to acceleration. These changes are above and below the nominal capacitance whose typical values are 2 to 3 pF. The differential capacitance ΔC is the absolute value of C_1 and C_2 difference is the measure of acceleration. The maximum value of ΔC will be 0.5 to 0.6 pF for full scale range of the accelerometer. The capacitance change at its minimum resolution is of the order of less than a femto Farad. These small values of capacitances are very critical for capacitance to voltage conversion, where parasitic capacitances and static voltage coupling within the package adversely effects the output voltage variation which in turn effect the desired resolution of the sensor.

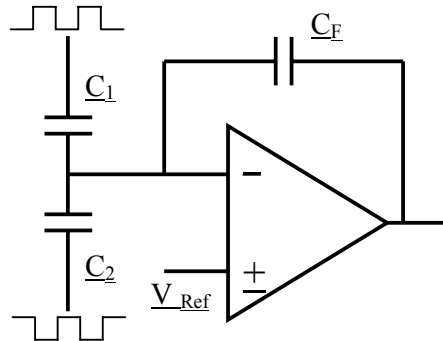


Figure 8. Signal Conversion Scheme – Capacitance to Voltage conversion electronics

The C-V conversion scheme is shown in the figure 8. The charge amplifier with feed back capacitor C_F is used [4]. The output voltage is proportional to the ΔC . The sensor is packaged in TO-8 package and populated along with charge amplifier on a single layer PCB. The functional test set up of differential capacitive accelerometer is shown in figure 9.

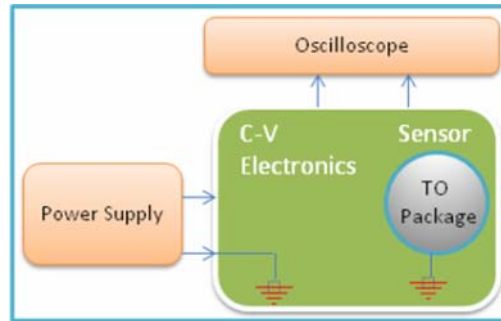


Figure 9. Functional Test Setup of Differential Capacitive Accelerometer

3.2 Specifications

Acceleration;

Range : ± 30 g

Resolution : 50 mg

Scale factor : 1 mg = 20 mV

Nominal output at '0'g : 2.25 V typical

Input supply : + 5 V DC

3.3 Test Results

The functional test of differential capacitive accelerometer is carried out and the performance of the device output voltage variation observed on oscilloscope with zero acceleration. The fluctuation in the output voltage is observed even for steady measurand. The variation in the output voltage is very large and measured as 56 mV peak to peak, which is out of the permissible limit levels. The oscilloscope output voltage variation plot is shown in the figure 10 along with the measured numerical values.

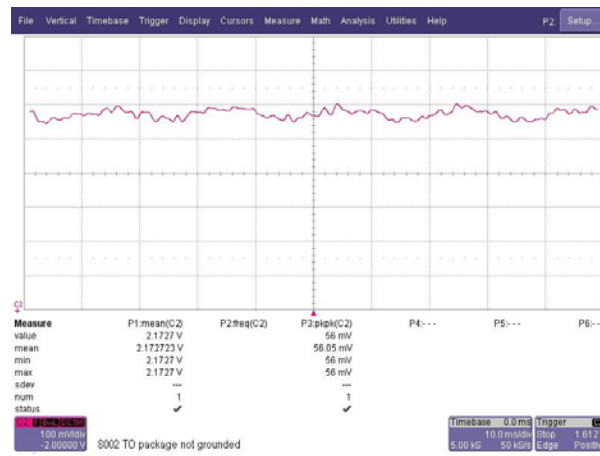


Figure 10. Differential Capacitive Accelerometer output voltage variation plot

3.4 Observations

- a) The variation in the output voltage is very large as shown in the above plot and the measured peak to peak voltage is 56 mV, which corresponds to the 'g.' level equivalent to ± 1400 mg
- b) The C - V conversion electronics scheme is so sensitive to sense the ΔC variations in the order of femto Farads.
- c) The variation in the output is also observed due to the parasitic capacitance effects, i.e., when the operator's hand is moved near the device.
- d) The sensor is packaged in metallic TO-8 package and populated along with charge amplifier on a PCB.

3.5 Analysis

- a) The differential capacitive accelerometer was found encapsulated in a plastic package (enclosure), which was contributing to accumulate the static charge.
- b) Ground plane of the PCB card was not connected / terminated to the chassis ground.
- c) The sensor package TO-8, metal cap / body was not grounded.
- d) Input power to the unit was 5 V, DC floating supply.
- e) Bare wires were used for both input power supply lines and for output monitoring.
- f) Oscilloscope earth point was not properly grounded.

3.6 EMI control methods (Solutions)

- a) The sensor package is encapsulated in a metallic enclosure (aluminium material of 3mm thickness), without any anodisation coating for better conductivity.
- b) Ensured the grounding of sensor package TO - 8 metal cap to the ground plane of the PCB card.
- c) PCB card ground plane is connected / terminated to the metallic chassis of device for obtaining the equipotential plane
- d) All the bare wires used were replaced with shielded twisted pairs
- e) Ensured the proper grounding of the oscilloscope earth point to the nearest earth point.

3.7 Test results after EMI hardening

After implementing the above solutions the functional test is repeated with the zero acceleration as per the test requirements and monitored the variation in output voltage on the oscilloscope. The voltage variation plot (captured from the oscilloscope picture) along with the numerical values is shown in figure 11. The measured output voltage is very much closer to the required or specified limits of voltage. The maximum variation of voltage is observed as 3mVp-p, after EMI hardening, against the 56mVp-p before it is EMI hardened. The overall improvement achieved is about 25.42 dB.

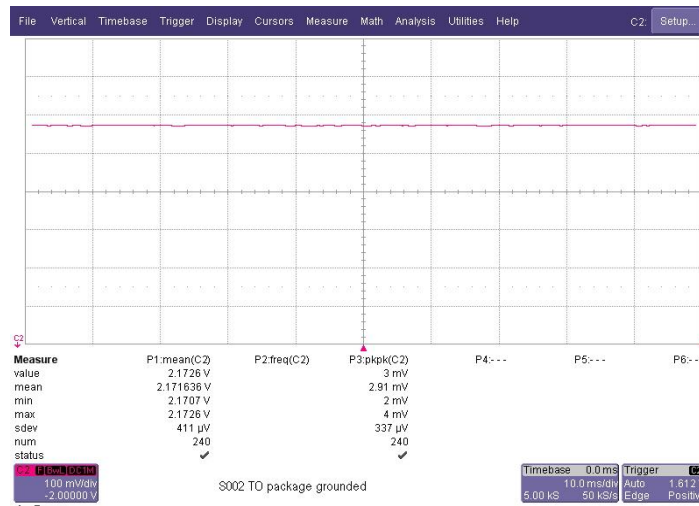


Figure 11. Differential Capacitive Accelerometer output voltage variation plot after EMI hardening

The redundant variations in the output voltage, i.e. ± 28 mV (56mV p-p), which corresponding to ± 1400 mg in terms of measurand has been reduced to ± 75 mg by limiting output variation within ± 1.5 mV (3mV p-p). The performance of the device can be further improved by using good shielded twisted pair cables and good packaging (metallic enclosure).

4. Conclusion

The intra system EMI coupling problems of devices, gyro and differential capacitive accelerometer have been resolved and achieved the specified functional performance requirements by identifying the sources of noise and incorporating appropriate EMI control techniques, without any major modification in the equipment design. Hence, it is very essential to identify and resolve the EMI problems during design and development of a product by following systematic approach, proper analysis and implementing the necessary EMI mitigation techniques. This will help in achieving EMC by design and also saves the cost and time of the product.

Acknowledgements

The authors are very much grateful to Shri. S.K.Ray, Outstanding Scientist, Director, RCI, and Shri. W.N. Raghupathy, Associate Director, RCI, for their motivation in development of these sensors indigenously. Thanks are also due to Shri. D.S.Reddy, Director, SINT (E), Shri. K. Rambabu, Dean, ELOIRA, Shri. G. Sateesh Reddy, Director, ISG, Shri. L. Sobhan Kumar, Director, Control Systems and for their continuous encouragement in solving the problems in time.

REFERENCES

- [1] Anthony Lawrence, “*Modern Inertial Technology Navigation, Guidance and Control*” Second Edition
- [2] Y.V. Bakin, G.N. Ziouzev and M.B. Lioumirski “*Optical Gyros and their Application*”, (Laser Gyro with Total Reflection Prisms, RTO AGARDograph 339)
- [3] Tai ran hsu, “*MEMS and Microsystems design and manufacture*”.
- [4] MSY Siva Prasad, G. Ravi, B. Sudha Rani, “*Design and Development of Differential Capacitive Accelerometer*”, ISSS-MEMS 2006 Conference, RCI, DRDO, Hyderabad.